

Controller Design for Euler-Bernoulli Smart Structures Using Robust Decentralized POF via Reduced Order Modeling

T.C. Manjunath¹, *Student Member IEEE*, and B. Bandyopadhyay², *member IEEE*

Abstract—This paper features the proposed modeling and design of a Robust Decentralized Periodic Output Feedback (RDPOF) control technique for the active vibration control of smart flexible multimodel Euler-Bernoulli cantilever beams for a multivariable (MIMO) case by retaining the first 6 vibratory modes. The beam structure is modeled in state space form using the concept of piezoelectric theory, the Euler-Bernoulli beam theory and the Finite Element Method (FEM) technique by dividing the beam into 4 finite elements and placing the piezoelectric sensor / actuator at two finite element locations (positions 2 and 4) as collocated pairs, i.e., as surface mounted sensor / actuator, thus giving rise to a multivariable model of the smart structure plant with two inputs and two outputs. Five such multivariable models are obtained by varying the dimensions (aspect ratios) of the aluminum beam, thus giving rise to a multimodel of the smart structure system. Using model order reduction technique, the reduced order model of the higher order system is obtained based on dominant eigen value retention and the method of Davison. RDPOF controllers are designed for the above 5 multivariable-multimodel plant. The closed loop responses with the RDPOF feedback gain and the magnitudes of the control input are observed and the performance of the proposed multimodel smart structure system with the controller is evaluated for vibration control.

Keywords—Smart structure, Euler-Bernoulli beam theory, Periodic output feedback control, Finite Element Method, State space model, SISO, Embedded sensors and actuators, Vibration control, Reduced order model

I. INTRODUCTION

PIEZOELECTRIC materials are capable of altering the structure's response through sensing, actuation and control. Piezoelectric elements can be incorporated into a laminated composite structure, either by embedding it or by mounting it onto the surface of the host structure [7]. Vibration control of any system is always a formidable challenge for any control system designer. Active control of

vibrations relieves a designer from strengthening the structure from dynamic forces and the structure itself from extra weight and cost. The need for intelligent structures such as smart structures arises from the high performance requirements of such structural members in numerous applications. Intelligent structures are those which incorporate actuators and sensors that are highly integrated into the structure and have structural functionality, as well as highly integrated control logic, signal conditioning and power amplification electronics [3].

A vibration control system consists of 4 parts, viz., actuator, controller, sensor and the system or the plant, which is to be controlled. When an external force f_{ext} is applied to the beam, it is subjected to vibrations. These vibrations should be suppressed. Fully active actuators like the Piezoelectrics, MR Fluids, Piezoceramics, ER Fluids, Shape Memory Alloys, PVDF, etc., can be used to generate a secondary vibrational response in a mechanical system. This could reduce the overall response of the system plant by the destructive interference with the original response of the system, caused by the primary source of vibration [2], [3], [10], [13].

Extensive research in modeling of piezoelectric materials in building actuators and sensors for structure is reported. Investigations of Crawley and Luis [3] emphasized on the derivation of sensor / actuator modeling of piezo-electric materials. Moreover, the control analysis of cantilever beams using these sensors / actuators have been studied by Bailey and Hubbard [2]. Culshaw [7] gave a brief introduction to the concept of smart structure, its benefits and applications. Hanagud, *et al.*, [13] developed a Finite Element Model (FEM) for an active beam with many distributed piezoceramic sensors / actuators coupled by signal conditioning systems and applied optimal output feedback control.

Fanson and Caughey [10] performed some experiments on a beam with piezoelectrics using positive position feedback. Hwang and Park [12] presented a FE model for piezoelectric sensors and actuators. Balas [16] presented the feedback control of flexible structures. Choi *et al.* [8] discussed about the control techniques of flexible structures using distributed piezoelectric sensors / actuators. Feedback control of vibrations in mechanical systems has numerous applications, like in aircrafts, active noise and shape control, acoustic control, control of antennas, earthquake, structural health monitoring, control of space structures and in the control of

¹Mr. T. C. Manjunath is a Research Scholar in the Interdisciplinary Programme for Systems and Control Engineering, Indian Institute of Technology Bombay, Powai, Mumbai-400076, Maharashtra, India. (Corresponding author phone : +91 22 25780263 / 25767884 ; Fax: +91 22 25720057 ; E-mail: tmanju@sc.iitb.ac.in, tmanjunath@gmail.com, URL : <http://www.sc.iitb.ac.in/~tmanju>).

²Dr. B. Bandyopadhyay is with the Systems and Control Engineering of IIT Bombay, Mumbai-76, Maharashtra, India and is currently a Professor.

(Email : bijnan@ee.iitb.ac.in, URL : <http://www.sc.iitb.ac.in/~bijnan>).

flexible manipulators. Fault tolerant control of smart structures using POF when one of the actuator fails to function was proposed in [19]. Manjunath and Bandyopadhyay proposed a AVC scheme for the best location (and for the best model) of the sensor / actuator pair on a beam modeled with Euler-Bernoulli beam theory in [17] and [18].

The outline of the paper is as follows. A brief review of related literature was given in Section 1. Section 2 gives a brief introduction to the modeling technique (sensor / actuator model, finite element model, state space model) of the smart flexible cantilever beam for a multivariable case with two inputs and two outputs. A brief review of the controlling technique, viz., the periodic output feedback control technique, multimodel synthesis, design of the LMI formulation, RDPOF design, model order reduction technique and the design of the robust decentralized periodic output feedback controller to control the first 6 modes of vibration of the system via reduced order modeling is discussed in section 4. The simulation results are shown in section 5 followed by the concluding section.

II. MATHEMATICAL MODELING OF SMART BEAM

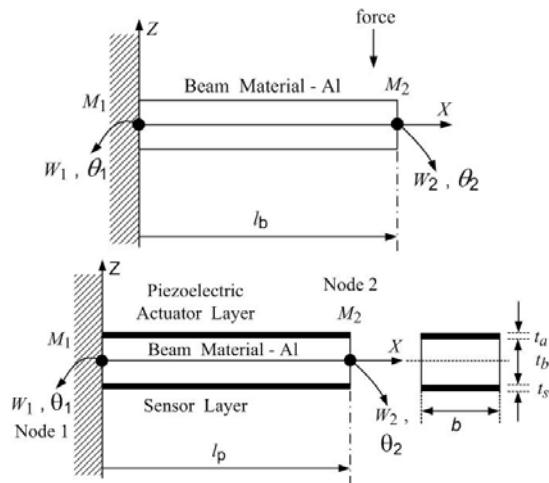


Fig. 1 A regular flexible beam and a smart flexible beam.
 F_1 and F_2 : Forces at node 1 and 2, M_1 and M_2 : Moments at node 1 and 2, l_b : Length of beam, l_p : Length of piezo-layer

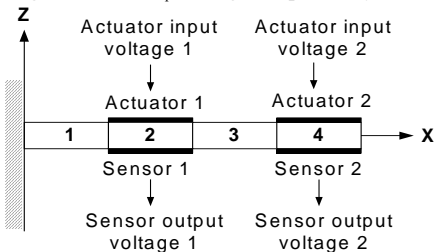


Fig. 2 A smart flexible beam divided into 4 FE with piezo patches placed at even FE positions 2 and 4

Consider a flexible cantilever beam made of aluminum bonded with piezoelectric sensor / actuator all along the length of the beam as shown in Fig. 1. The dimensions and properties of the flexible beam and piezoelectric sensor / actuator are given in Tables I and II respectively. The flexible

cantilever beam as shown in Fig. 1 is divided into a number of finite elements viz., 4 as shown in Fig. 2. The piezoelectric sensor / actuator is bonded to the master structure at finite element positions numbering 2 and 4, thus giving rise to a Multiple Input Multiple Output (MIMO) system with 2 actuator inputs u_1, u_2 to the actuators and 2 sensor outputs, y_1, y_2 from the sensors.

TABLE I
 PHYSICAL PARAMETERS
 PROPERTIES OF THE FLEXIBLE CANTILEVER BEAM ELEMENT

| Parameter (with units) | Symbol | Numerical values |
|--------------------------------------|-----------------|---|
| Total length (m) | l_b | 0.5 |
| Width (m) | b | 0.024 |
| Young's modulus (GPa) | E_b | 193.06 |
| Density (kg / m^3) | ρ_b | 8030 |
| Constants used in C^* | α, β | 0.001, 0.0001 |
| Thickness | t_b | Varying from 0.5 mm to 1 mm, i.e., to give 5 models |

TABLE II
 PROPERTIES OF THE (PZT) PIEZO - SENSOR / ACTUATOR

| Parameter (with units) | Symbol | Numerical values |
|---|------------|------------------------|
| Length (m) | l_p | 0.125 |
| Width (m) | b | 0.024 |
| Thickness (mm) | t_a, t_s | 0.5 |
| Young's modulus (GPa) | E_p | 68 |
| Density (kg / m^3) | ρ_p | 7700 |
| Piezoelectric stress constant (VmN^{-1}) | g_{31} | 10.5×10^{-13} |
| Piezo strain constant (m / V) | d_{31} | 125×10^{-12} |

A. Modeling of Regular and Piezo Elements of Beam

To start with, we consider the modeling of the regular beam element and the piezoelectric beam element as shown in the Fig. 1. The dynamic model for the smart structure is developed using the Finite Element Method (FEM) [12], [24]. The smart cantilever beam model is developed using a piezoelectric beam element, which includes the sensor and actuator dynamics and a regular beam element based on Euler-Bernoulli theory assumptions. The piezoelectric beam element is used to model the regions where the piezoelectric element is bonded as sensor / actuator and the rest of the structure is modeled by the regular beam elements.

In modeling and analysis of the smart beam, the following assumptions are made. The perfect bonding or the adhesive between the beam and the sensor / actuator and the thin film electrode surfaces have been assumed to add no mass or stiffness to the sensor / actuator, i.e., neglected. The cable capacitance between sensor and signal-conditioning device has been considered negligible and the temperature effects

have been neglected. The signal conditioning device gain (G_c) is assumed as 100. The free vibration characteristics of a flexible beam is governed by the following fourth order differential equation [20], [25]

$$c^2 \frac{\partial^4 w(x,t)}{\partial x^4} + \frac{\partial^2 w(x,t)}{\partial t^2} = 0, \quad (1)$$

where w is the transverse displacement of the beam and is a function x and t , x being the distance of the local coordinate from the fixed end, t being the time and c is a constant which is given by $\sqrt{EI/\rho A}$.

E, I, ρ and A are the young's modulus, moment of inertia, mass density and area of the beam respectively. When a system vibrates, it undergoes to and fro motion and so all positions vary with time and therefore, the system has velocities and accelerations. Mass times acceleration as inertia force appears in the governing differential equation of the beam which is given in Eq. (1), i.e., the equation of motion involves a fourth order derivative w.r.t. x and a second order derivative w.r.t. time.

The piezoelectric element is obtained by sandwiching the regular beam element between two thin piezoelectric layers as shown in Fig. 2. The bottom layer is acting as a sensor and the top layer acts as an actuator. The beam element is assumed to have two structural DOF (w, θ) at each nodal point and an electrical DOF: a transverse deflection and an angle of rotation or slope. Since the voltage is constant over the electrode, the number of electrical DOF is one for each element.

The electrical DOF is used as a sensor voltage or actuator voltage when the piezoelectric material attached to the structure behaves as sensor or actuator. Corresponding to the 2 DOF, a transverse shear force and a bending moment acts at each nodal point. At each nodal point, counteracting moments induced by the piezoelectric actuators will be acting. The bending moment resulting from the applied voltage to the actuator adds a positive finite element being the moment at node 1 while subtracting it at node 2.

The deflection behavior of the beam element is best described by a displacement function $W(x)$, which is the solution of Eq. (1). It is desirable that this function satisfies the differential equation of equilibrium for the beam element. The solution of the Eq. (1) is assumed as a cubic polynomial function of x given by [20], [25]

$$W(x) = a_1 + a_2x + a_3x^2 + a_4x^3, \quad (2)$$

where the constants a_1 to a_4 are obtained using the boundary conditions of the beam at the nodal points (fixed end and free end) as

$$\begin{bmatrix} a_1 \\ a_2 \\ a_3 \\ a_4 \end{bmatrix} = \frac{1}{l_b^3} \begin{bmatrix} l_b^3 & 0 & 0 & 0 \\ 0 & l_b^3 & 0 & 0 \\ -3l_b & -2l_b^2 & 3l_b & -l_b^2 \\ 2 & l_b & -2 & l_b \end{bmatrix} \begin{bmatrix} w_1 \\ \theta_1 \\ w_2 \\ \theta_2 \end{bmatrix}. \quad (3)$$

where w_1, θ_1 and w_2, θ_2 are the DOF's at the node 1 (fixed end) and node 2 (free end) respectively.

The Eq. (2) is rearranged in the final form as

$$[W(x)] = [\mathbf{n}^T][\mathbf{q}], \quad (4)$$

where $[\mathbf{n}^T]$ gives the shape functions of the beam $f_i(x)$, $i = 1, \dots, 4$ as

$$[\mathbf{n}^T] = [f_1(x) \quad f_2(x) \quad f_3(x) \quad f_4(x)], \quad (5)$$

where

$$\mathbf{n} = \begin{bmatrix} 1 - 3\frac{x^2}{l_b^2} + 2\frac{x^3}{l_b^3} \\ x - 2\frac{x^2}{l_b} + \frac{x^3}{l_b^2} \\ 3\frac{x^2}{l_b^2} - 2\frac{x^3}{l_b^3} \\ -\frac{x^2}{l_b} + \frac{x^3}{l_b^2} \end{bmatrix}, \quad (6)$$

where x is the local axial coordinate of the finite element node from the fixed end, l_b being the length of the beam and \mathbf{q} is the vector of displacements and slopes (nodal displacement vector) and is given by

$$\mathbf{q} = \begin{bmatrix} w_1 \\ \theta_1 \\ w_2 \\ \theta_2 \end{bmatrix} \quad (7)$$

for the beam shown in Fig. 1. The displacement, its first, second spatial derivatives and its time derivative in matrix form is given by $W(x), W'(x), W''(x)$ and $\dot{W}(t)$ and is given by

$$[W'(x)] = [\mathbf{n}_2^T][\mathbf{q}],$$

$$\frac{\partial W}{\partial x} = [f_1'(x) \quad f_2'(x) \quad f_3'(x) \quad f_4'(x)] \begin{bmatrix} w_1 \\ \theta_1 \\ w_2 \\ \theta_2 \end{bmatrix}, \quad (8)$$

$$[W''(x)] = [\mathbf{n}_1^T][\mathbf{q}],$$

$$\frac{\partial^2 W}{\partial x^2} = [f_1''(x) \quad f_2''(x) \quad f_3''(x) \quad f_4''(x)] \begin{bmatrix} w_1 \\ \theta_1 \\ w_2 \\ \theta_2 \end{bmatrix}, \quad (9)$$

$$[\dot{W}(x)] = [\mathbf{n}_3^T][\dot{\mathbf{q}}];$$

$$\frac{\partial W(x)}{\partial t} = [f_1(x) \quad f_2(x) \quad f_3(x) \quad f_4(x)] \begin{bmatrix} \dot{w}_1 \\ \dot{\theta}_1 \\ \dot{w}_2 \\ \dot{\theta}_2 \end{bmatrix}. \quad (10)$$

B. Piezoelectric Strain Rate Sensors And Actuators

The linear piezoelectric coupling [22] between the elastic field and the electric field is expressed by the direct and the converse piezoelectric equations as

$$D = dT + \varepsilon^T E, \quad S = s^E T + d E, \quad (11)$$

where T is the stress, S is the strain, E is the electric field, D is the dielectric displacement, ε is the permittivity of the medium, s^E is the compliance of the medium and d is the piezoelectric constant.

C. Sensor Equation

The direct piezoelectric equation is used to calculate the output charge created by the strain in the structure [20], [25]. Since no external field is applied to the sensor layer, the electric displacement developed on the sensor surface is directly proportional to the strain acting on the sensor. If the poling is done along the thickness direction of the sensors with the electrodes on the upper and lower surfaces, the electric displacement is given as

$$D_z = d_{31} * E_p \varepsilon_x = e_{31} \varepsilon_x, \quad (12)$$

where e_{31} is the piezoelectric stress / charge constant, E_p is the Young's modulus and ε_x is the strain of the testing structure at a point on the beam.

The total charge $Q(t)$ developed on the sensor surface is the spatial summation of all the point charges developed on the sensor layer. Since the current $i(t) = \frac{dQ(t)}{dt}$ suggests that the closed-circuit current signal generated in a piezoelectric lamina is proportional to the strain rate of the testing structure, we obtain

$$i(t) = z e_{31} b \int_0^{l_p} \mathbf{n}_1^T \dot{\mathbf{q}} dx, \quad (13)$$

where $z = \frac{t_b}{2} + t_a$, b is the width of the beam, l_p being the length of the piezo-sensor and \mathbf{n}_1^T is the second spatial derivative of shape function of the flexible beam. This current is converted into the open circuit sensor voltage V^s using a signal-conditioning device with the gain G_c and applied to the actuator with the controller gain K_c . The sensor output voltage is obtained as

$$V^s(t) = G_c e_{31} z b \int_0^{l_p} \mathbf{n}_1^T \dot{\mathbf{q}} dx, \quad (14)$$

which is nothing but the signal conditioning gain G_c multiplied by the closed circuit current $i(t)$ generated by the piezoelectric lamina. Substituting for \mathbf{n}_1^T from Eq. (9) and $\dot{\mathbf{q}}$ from Eq. (10) and simplifying, we get the sensor voltage for

a two node finite element of the beam as

$$V^s(t) = \begin{bmatrix} 0 & -G_c e_{31} z b & 0 & G_c e_{31} z b \end{bmatrix} \begin{bmatrix} \dot{w}_1 \\ \dot{\theta}_1 \\ \dot{w}_2 \\ \dot{\theta}_2 \end{bmatrix} \\ = G_c e_{31} z b * \begin{bmatrix} 0 & -1 & 0 & 1 \end{bmatrix} \begin{bmatrix} \dot{w}_1 \\ \dot{\theta}_1 \\ \dot{w}_2 \\ \dot{\theta}_2 \end{bmatrix}, \quad (15)$$

which can be further expressed as a scalar-vector product

$$V^s(t) = \mathbf{p}^T \dot{\mathbf{q}}, \quad (16)$$

where $\dot{\mathbf{q}}$ is the time derivative of the modal coordinate vector \mathbf{q} , \mathbf{p}^T is a constant vector which depends on the type of sensor, its characteristics and its location on the beam. Note that the sensor output is a function of the second spatial derivative of the mode shape. This sensor voltage is given as input to the controller and the output of the controller (which is nothing but the control input to the actuator, i.e., the actuator voltage) is the controller gain K_c multiplied by the sensor voltage $V^s(t)$. Thus, the input voltage to the actuator $V^a(t)$ is given by

$$V^a(t) = K_c V^s(t). \quad (17)$$

Substituting for $V^s(t)$ from Eq. (14) in Eq. (17), we get

$$V^a(t) = K_c G_c e_{31} z b \int_0^{l_p} \mathbf{n}_1^T \dot{\mathbf{q}} dx. \quad (18)$$

D. Actuator Equation

The actuator strain is derived from the converse piezoelectric equation. The strain developed ε_a on the actuator layer is given by [20], [25]

$$\varepsilon_a = d_{31} E_f, \quad (19)$$

where d_{31} and E_f are the piezo strain constant and the electric field respectively. When the input to the piezoelectric actuator $V^a(t)$ is applied in the thickness direction t_a , the electric field, E_f which is the voltage applied $V^a(t)$ divided by the thickness of the actuator t_a ; and the stress, σ_a which is the actuator strain multiplied by the young's modulus E_p of the piezo actuator layer are given by

$$E_f = \frac{V^a(t)}{t_a} \quad (20)$$

and

$$\sigma_a = E_p d_{31} \frac{V^a(t)}{t_a}. \quad (21)$$

The resultant moment M_A acting on the beam is determined by integrating the stress throughout the structure thickness as

$$M_A = E_p d_{31} \bar{z} V^a(t), \quad (22)$$

where $\bar{z} = \frac{(t_a + t_b)}{2}$, is the distance between the neutral axis of the beam and the piezoelectric layer. Finally, the control force applied by the actuator is obtained as

$$\mathbf{f}_{ctrl} = E_p d_{31} b \bar{z} \int_{l_p} \mathbf{n}_2 dx V^a(t) \quad (23)$$

or can be expressed as a scalar vector product as

$$\mathbf{f}_{ctrl} = \mathbf{h} V^a(t) = \mathbf{h} u(t), \quad (24)$$

where \mathbf{n}_2^T is the first spatial derivative of the shape function of the flexible beam, \mathbf{h}^T is a constant vector which depends on the type of actuator and its location on the beam, given by $\mathbf{h} = [-E_p d_{31} b \bar{z} \quad 0 \quad E_p d_{31} b \bar{z} \quad 0]$ and $u(t)$ is nothing but the control input to the actuator, i.e., $V^a(t)$ from the controller. If any external forces described by the vector \mathbf{f}_{ext} are acting on the beam, then the total force vector becomes

$$\mathbf{f}^t = \mathbf{f}_{ext} + \mathbf{f}_{ctrl}. \quad (25)$$

E. Dynamic Equation of Smart Structure

The strain energy U and the kinetic energy T for the beam element with uniform cross section in bending is [20], [25]

$$U = \frac{E_b I_b}{2} \int_{l_b} \left[\frac{\partial^2 w}{\partial x^2} \right]^2 dx = \frac{E_b I_b}{2} \int_{l_b} [w''(x,t)]^T [w''(x,t)] dx, \quad (26)$$

$$T = \frac{\rho_b A_b}{2} \int_{l_b} [\dot{w}(x,t)]^2 dx = \frac{\rho_b A_b}{2} \int_{l_b} [\dot{w}(x,t)]^T [\dot{w}(x,t)] dx. \quad (27)$$

The equation of motion of the regular beam element is obtained by the Lagrangian equation for the regular beam element as

$$\frac{d}{dt} \left[\frac{\partial T}{\partial \dot{q}_i} \right] + \left[\frac{\partial U}{\partial q_i} \right] = [F_i], \quad (28)$$

which after simplification yields as

$$M^b \ddot{q} + K^b q = f^b(t), \quad (29)$$

where

$$[M^b] = \rho_b A_b \int_{l_b} [\mathbf{n}_3]^T [\mathbf{n}_3] dx, \quad (30)$$

$$[M_{ij}^b] = \rho_b A_b \int_{l_b} f_i(x) f_j(x) dx \quad (31)$$

and

$$[K^b] = E_b I_b \int_{l_b} [\mathbf{n}_1]^T [\mathbf{n}_1] dx, \quad (32)$$

$$[K_{ij}^b] = E_b I_b \int_{l_b} f_i''(x) f_j''(x) dx. \quad (33)$$

Finally, after simplification, we get

$$M^b = \frac{\rho_b A_b l_b}{420} \begin{bmatrix} 156 & 22l_b & 54 & -13l_b \\ 22l_b & 4l_b^2 & 13l_b & -3l_b^2 \\ 54 & 13l_b & 156 & -22l_b \\ -13l_b & -3l_b^2 & -22l_b & 4l_b^2 \end{bmatrix} \quad (34)$$

and

$$K^b = \frac{E_b I_b}{l_b} \begin{bmatrix} 12/l_b^2 & 6/l_b & -12/l_b^2 & 6/l_b \\ 6/l_b & 4 & -6/l_b & 2 \\ -12/l_b^2 & -6/l_b & 12/l_b^2 & -6/l_b \\ 6/l_b & 2 & -6/l_b & 4 \end{bmatrix}, \quad (35)$$

where M^b , K^b are the local mass matrix, the local stiffness matrix of the regular beam element.

Similarly, the lagrangian equation of motion for the piezoelectric beam element is obtained as

$$M^p \ddot{q} + K^p q = f^p(t), \quad (36)$$

where M^p and K^p are the piezoelectric beam element mass matrix and stiffness matrix and are given as

$$M^p = \frac{\rho A l_p}{420} \begin{bmatrix} 156 & 22l_p & 54 & -13l_p \\ 22l_p & 4l_p^2 & 13l_p & -3l_p^2 \\ 54 & 13l_p & 156 & -22l_p \\ -13l_p & -3l_p^2 & -22l_p & 4l_p^2 \end{bmatrix}, \quad (37)$$

$$K^p = \frac{EI}{l_p} \begin{bmatrix} 12/l_p^2 & 6/l_p & -12/l_p^2 & 6/l_p \\ 6/l_p & 4 & -6/l_p & 2 \\ -12/l_p^2 & -6/l_p & 12/l_p^2 & -6/l_p \\ 6/l_p & 2 & -6/l_p & 4 \end{bmatrix}, \quad (38)$$

where

$$EI = E_b I_b + 2E_p I_p, \quad (39)$$

$$I_p = \frac{1}{12} b t_a^3 + b t_a \left(\frac{t_a + t_b}{2} \right)^2, \quad (40)$$

and

$$\rho A = b(\rho_b t_b + 2\rho_p t_a). \quad (41)$$

The dynamic equation of the smart structure is obtained by using both the regular and piezoelectric beam elements given by Eqs. (29) and (36). The mass and stiffness of the bonding or the adhesive between the master structure and the sensor / actuator pair is neglected. The mass and stiffness of the entire beam, which is divided into 4 finite elements is assembled using the FEM technique [12], [24] and the assembled matrices (global matrices), \mathbf{M} and \mathbf{K} are obtained. The equation of motion of the smart structure is finally given by

$$\mathbf{M} \ddot{\mathbf{q}} + \mathbf{K} \mathbf{q} = \mathbf{f}_{ext} + \mathbf{f}_{ctrl} = \mathbf{f}^t, \quad (42)$$

where \mathbf{M} , \mathbf{K} , \mathbf{q} , \mathbf{f}_{ext} , \mathbf{f}_{ctrl} , \mathbf{f}^t are the global mass matrix, global stiffness matrix of the smart beam, the vector of displacements and slopes, the external force applied to the beam, the controlling force from the actuator and the total force coefficient vector respectively. The mass matrix \mathbf{M} ,

stiffness matrix \mathbf{K} and the control force vector \mathbf{h}^T in the system equation can be varied by changing the position and number of regular and piezoelectric beam elements.

The generalized coordinates are introduced into the Eq. (42) using a transformation $\mathbf{q} = \mathbf{T} \mathbf{g}$ in order to reduce it further such that the resultant equation represents the dynamics of the first 6 vibratory modes ω_1 to ω_6 of the smart flexible cantilever beam. \mathbf{T} is the modal matrix containing the eigen vectors representing the first 6 vibratory modes. This method is used to derive the uncoupled equations governing the motion of the free vibrations of the system in terms of principal coordinates by introducing a linear transformation between the generalized coordinates \mathbf{q} and the principal coordinates \mathbf{g} . The Eq. (42) now becomes

$$\mathbf{M} \mathbf{T} \ddot{\mathbf{g}} + \mathbf{K} \mathbf{T} \mathbf{g} = \mathbf{f}_{ext} + \mathbf{f}_{ctrl 1} + \mathbf{f}_{ctrl 2}, \quad (43)$$

where $\mathbf{f}_{ctrl 1}$ and $\mathbf{f}_{ctrl 2}$ are the control force coefficient vectors to the actuators from the controller.

Multiplying Eq. (43) by \mathbf{T}^T on both sides and further simplifying, we get

$$\mathbf{M}^* \ddot{\mathbf{g}} + \mathbf{K}^* \mathbf{g} = \mathbf{f}_{ext}^* + \mathbf{f}_{ctrl 1}^* + \mathbf{f}_{ctrl 2}^*, \quad (44)$$

where $\mathbf{M}^* = \mathbf{T}^T \mathbf{M} \mathbf{T}$, $\mathbf{K}^* = \mathbf{T}^T \mathbf{K} \mathbf{T}$, $\mathbf{f}_{ext}^* = \mathbf{T}^T \mathbf{f}_{ext}$, $\mathbf{f}_{ctrl i}^* = \mathbf{T}^T \mathbf{f}_{ctrl i}$ $i = 1$ to 2 .

\mathbf{M}^* , \mathbf{K}^* , \mathbf{f}_{ext}^* , $\mathbf{f}_{ctrl 1}^*$, $\mathbf{f}_{ctrl 2}^*$ represents the generalized mass matrix, the generalized stiffness matrix, the generalized external force vector and the generalized control force vectors respectively.

The generalized structural modal damping matrix \mathbf{C}^* (Rayleigh proportional damping) is introduced into the Eq. (44) by using

$$\mathbf{C}^* = \alpha \mathbf{M}^* + \beta \mathbf{K}^*, \quad (45)$$

where α and β are the damping constant respectively.

The dynamic equation of the smart flexible cantilever beam developed is as

$$\mathbf{M}^* \ddot{\mathbf{g}} + \mathbf{C}^* \dot{\mathbf{g}} + \mathbf{K}^* \mathbf{g} = \mathbf{f}_{ext}^* + \mathbf{f}_{ctrl}^*, \quad (46)$$

where $\mathbf{f}_{ctrl}^* = \mathbf{f}_{ctrl 1}^* + \mathbf{f}_{ctrl 2}^*$.

F. State Space Model of the Smart Structure

The state space model of the smart flexible cantilever beam is obtained as follows [20], [25]. Let

$$\mathbf{g} = \begin{bmatrix} x_1 \\ x_2 \\ \vdots \\ x_6 \end{bmatrix} \text{ and } \dot{\mathbf{g}} = \begin{bmatrix} \dot{x}_7 \\ \dot{x}_8 \\ \vdots \\ \dot{x}_{12} \end{bmatrix}. \quad (47)$$

$$\therefore, \dot{\mathbf{g}} = \begin{bmatrix} \dot{x}_1 \\ \dot{x}_2 \\ \vdots \\ \dot{x}_6 \end{bmatrix} = \begin{bmatrix} x_7 \\ x_8 \\ \vdots \\ x_{12} \end{bmatrix} \text{ and } \ddot{\mathbf{g}} = \begin{bmatrix} \ddot{x}_7 \\ \ddot{x}_8 \\ \vdots \\ \ddot{x}_{12} \end{bmatrix}. \quad (48)$$

Thus,

$$\begin{aligned} \dot{x}_1 &= x_7, \quad \dot{x}_2 = x_8, \quad \dot{x}_3 = x_9, \\ \dot{x}_4 &= x_{10}, \quad \dot{x}_5 = x_{11}, \quad \dot{x}_6 = x_{12}. \end{aligned} \quad (49)$$

and Eq. (46) now becomes

$$\mathbf{M}^* \begin{bmatrix} \dot{x}_7 \\ \dot{x}_8 \\ \dot{x}_9 \\ \dot{x}_{10} \\ \dot{x}_{11} \\ \dot{x}_{12} \end{bmatrix} + \mathbf{C}^* \begin{bmatrix} x_7 \\ x_8 \\ x_9 \\ x_{10} \\ x_{11} \\ x_{12} \end{bmatrix} + \mathbf{K}^* \begin{bmatrix} x_1 \\ x_2 \\ x_3 \\ x_4 \\ x_5 \\ x_6 \end{bmatrix} = \mathbf{f}_{ext}^* + \mathbf{f}_{ctrl}^*. \quad (50)$$

which can be further simplified as

$$\begin{bmatrix} \dot{x}_7 \\ \dot{x}_8 \\ \dot{x}_9 \\ \dot{x}_{10} \\ \dot{x}_{11} \\ \dot{x}_{12} \end{bmatrix} = -\mathbf{M}^{*-1} \mathbf{K}^* \begin{bmatrix} x_1 \\ x_2 \\ x_3 \\ x_4 \\ x_5 \\ x_6 \end{bmatrix} - \mathbf{M}^{*-1} \mathbf{C}^* \begin{bmatrix} x_7 \\ x_8 \\ x_9 \\ x_{10} \\ x_{11} \\ x_{12} \end{bmatrix} + \mathbf{M}^{*-1} \mathbf{f}_{ext}^* + \mathbf{M}^{*-1} \mathbf{f}_{ctrl}^*. \quad (51)$$

The generalized external force coefficient vector is

$$\mathbf{f}_{ext}^* = \mathbf{T}^T \mathbf{f}_{ext} = \mathbf{T}^T f r(t), \quad (52)$$

where $r(t)$ is the external force input (impulse disturbance) to the beam.

The generalized control force coefficient vector is

$$\mathbf{f}_{ctrl i}^* = \mathbf{T}^T f_{ctrl i} = \mathbf{T}^T \mathbf{h}_i V_i^a(t) = \mathbf{T}^T \mathbf{h}_i u_i(t), \quad i=1 \text{ to } 2, \quad (53)$$

where the voltages $V_i^a(t)$ are the input voltages to the actuators 1 and 2 from the controllers respectively, and are nothing but the control inputs $u_i(t)$ to the actuators, \mathbf{h}_i is a constant vector which depends on the actuator type, its position on the beam and is given by

$$\begin{aligned} \mathbf{h}_1 &= E_p d_{31} b \bar{z} [-1 \quad 1 \quad \dots \dots \dots 0 \quad 0]_{8 \times 1} \\ &= a_c [-1 \quad 1 \quad \dots \dots \dots 0 \quad 0] \end{aligned} \quad (54)$$

for one piezoelectric actuator element (say, for the piezo patch placed at the finite element position numbering 2), where $E_p d_{31} b \bar{z} = a_c$ being the actuator constant. So, using the Eqs. (52) and (53) in Eq. (51), the state space equation for the smart beam is represented as

$$\begin{bmatrix} \dot{x}_1 \\ \dot{x}_2 \\ \vdots \\ \dot{x}_{12} \end{bmatrix} = \begin{bmatrix} 0 & I \\ -\mathbf{M}^{*-1} \mathbf{K}^* & -\mathbf{M}^{*-1} \mathbf{C}^* \end{bmatrix}_{(12 \times 12)} \begin{bmatrix} x_1 \\ x_2 \\ \vdots \\ x_{12} \end{bmatrix}_{(12 \times 1)} + \begin{bmatrix} 0 & 0 \\ \mathbf{M}^{*-1} \mathbf{T}^T \mathbf{h}_1 & \mathbf{M}^{*-1} \mathbf{T}^T \mathbf{h}_2 \end{bmatrix}_{(12 \times 2)} \begin{bmatrix} u_1 \\ u_2 \end{bmatrix}_{(2 \times 1)} + \begin{bmatrix} 0 \\ \mathbf{M}^{*-1} \mathbf{T}^T \mathbf{f} \end{bmatrix}_{(12 \times 1)} r(t). \quad (55)$$

i.e., $\dot{\mathbf{X}} = \mathbf{A}x(t) + \mathbf{B}u(t) + \mathbf{E}r(t).$ (56)

The sensor voltage is taken as the output and its equation is modeled as

$$V_i^s(t) = \mathbf{p}_i^T \dot{\mathbf{q}} = y_i(t), \quad i=1,2, \quad (57)$$

where \mathbf{p}_i^T is a constant vector which depends on the piezoelectric sensor characteristics (i.e., the sensor constant S_c) and on the position of the sensor location on the beam. The constant vector for the sensor placed at finite element position numbering 4 is given by

$$\begin{aligned} \mathbf{p}_2^T &= G_c e_{31} z b [0 \quad 0 \quad \dots \quad -1 \quad 1]_{1 \times 8} \\ &= S_c [0 \quad 0 \quad \dots \quad -1 \quad 1], \end{aligned} \quad (58)$$

where $G_c e_{31} z b = S_c$ is the sensor constant.

Thus, the sensor output is given by

$$y(t) = \mathbf{p}^T \dot{\mathbf{q}} = \mathbf{p}^T \mathbf{T} \dot{\mathbf{g}} = \mathbf{p}^T \mathbf{T} \begin{bmatrix} \dot{x}_1 \\ \dot{x}_2 \\ \dot{x}_3 \\ \dot{x}_4 \\ \dot{x}_5 \\ \dot{x}_6 \end{bmatrix}, \quad (59)$$

which can be written as

$$\begin{bmatrix} y_1 \\ y_2 \end{bmatrix} = \begin{bmatrix} 0 & \mathbf{p}_1^T \\ 0 & \mathbf{p}_2^T \end{bmatrix}_{(2 \times 12)} \begin{bmatrix} x_1 \\ x_2 \\ \vdots \\ x_{12} \end{bmatrix}_{(12 \times 1)} \quad (60)$$

for a multivariable case with 2 inputs and 2 outputs. i.e.,

$$y(t) = \mathbf{C}^T x(t) + \mathbf{D}u(t). \quad (61)$$

The multivariable state space model (state equation and the output equation) of the smart structure developed for the system thus [20], [25], is given by

$$\begin{aligned} \dot{\mathbf{x}} &= \mathbf{A}x(t) + \mathbf{B}u(t) + \mathbf{E}r(t), \\ y(t) &= \mathbf{C}^T x(t) + \mathbf{D}u(t), \end{aligned} \quad (62)$$

with

$$\begin{aligned} \mathbf{A} &= \begin{bmatrix} 0 & I \\ -\mathbf{M}^{*-1} \mathbf{K}^* & -\mathbf{M}^{*-1} \mathbf{C}^* \end{bmatrix}_{(12 \times 12)}, \\ \mathbf{B} &= \begin{bmatrix} 0 & I \\ \mathbf{M}^{*-1} \mathbf{T}^T \mathbf{h}_1 & \mathbf{M}^{*-1} \mathbf{T}^T \mathbf{h}_2 \end{bmatrix}_{(12 \times 2)}, \\ \mathbf{C}^T &= \begin{bmatrix} 0 & \mathbf{p}_1^T \\ 0 & \mathbf{p}_2^T \end{bmatrix}_{(2 \times 12)}, \\ \mathbf{D} &= \text{a null matrix,} \\ \mathbf{E} &= \begin{bmatrix} 0 \\ \mathbf{M}^{*-1} \mathbf{T}^T \mathbf{f} \end{bmatrix}_{(12 \times 1)}, \end{aligned} \quad (63)$$

where $r(t), u(t), \mathbf{A}, \mathbf{B}, \mathbf{C}, \mathbf{D}, \mathbf{E}, x(t)$ and $y(t)$ represents the external force input, the control input, system matrix, input matrix, output matrix, transmission matrix, external load matrix, state vector, system output (sensor output).

By considering the thickness of the beam in the model 1 as 0.5 mm, thickness of the beam in model 2 as 0.6 mm, thickness of the beam in model 3 as 0.7 mm, thickness of the beam in the model 4 as 0.8 mm and thickness of the beam in the model 5 as 1 mm, 5 multivariable state space models (multi-model) of the same smart structure plant are obtained as shown in Eq. (62).

These 5 MIMO models give rise to a multimodel smart structure plant. Let $(\mathbf{A}_i, \mathbf{B}_i, \mathbf{C}_i, \mathbf{D}_i, \mathbf{E}_i); i=1,2,3,4,5$ be the state space matrices of the 5 models of the beam. State space model of the smart cantilever beam with sensor / actuator pair at element 2 and 4 for the model 1 for 6 modes is represented by Eq. (62) with

$$\begin{aligned} \mathbf{C}_1^T &= \begin{bmatrix} 0 & 0 & 0 & 0 & 0 & 0 & -0.0404 & -0.0453 \\ 0 & 0 & 0 & 0 & 0 & 0 & 0.2084 & -0.1783 \\ 0.0415 & -0.0044 & -0.0212 & -0.0200 \\ -0.1050 & 0.0455 & 0.1427 & -0.1254 \end{bmatrix}, \\ \mathbf{B}_1 &= \begin{bmatrix} 0 & 0 \\ 0 & 0 \\ 0 & 0 \\ 0 & 0 \\ 0 & 0 \\ 0 & 0 \\ 16.5924 & -21.3687 \\ -7.1011 & 25.4467 \\ 13.5529 & 15.3619 \\ -6.5758 & 9.1164 \\ -0.4503 & 3.9458 \\ -0.3630 & -0.4057 \end{bmatrix}; \mathbf{E}_1 = 10^3 \begin{bmatrix} 0 \\ 0 \\ 0 \\ 0 \\ 0 \\ 0 \\ -2.4449 \\ 1.6580 \\ 0.7635 \\ 0.4944 \\ 0.3082 \\ -0.1110 \end{bmatrix}, \quad (64) \\ \mathbf{D}_1 &= \text{Null matrix,} \end{aligned}$$

$$A_1 = 10^6 \begin{bmatrix} 0 & 0 & 0 & 0 & 0 & 0 \\ 0 & 0 & 0 & 0 & 0 & 0 \\ 0 & 0 & 0 & 0 & 0 & 0 \\ 0 & 0 & 0 & 0 & 0 & 0 \\ 0 & 0 & 0 & 0 & 0 & 0 \\ 0 & 0 & 0 & 0 & 0 & 0 \\ -2.992 & 0.0 & -0.0 & -0.0 & -0.0 & 0.0 \\ -0.0 & -1.082 & 0.0 & 0.0 & -0.0 & -0.0 \\ -0.0 & -0.0 & -0.2836 & -0.0 & 0.0 & -0.0 \\ 0.0 & 0.0 & -0.0 & -0.0661 & 0.0 & 0.0 \\ -0.0 & -0.0 & -0.0 & -0.0 & -0.0080 & 0.0 \\ -0.0 & -0.0 & 0.0 & -0.0 & 0.0 & -0.0001 \\ 0 & 0 & 0 & 0 & 0 & 0 \\ 0 & 0 & 0 & 0 & 0 & 0 \\ 0 & 0 & 0 & 0 & 0 & 0 \\ 0 & 0 & 0 & 0 & 0 & 0 \\ 0 & 0 & 0 & 0 & 0 & 0 \\ 0 & 0 & 0 & 0 & 0 & 0 \\ -0.0004 & 0.0 & -0.0 & -0.0 & -0.0 & 0.0 \\ -0.0 & -0.0002 & 0.0 & 0.0 & -0.0 & -0.0 \\ -0.0 & -0.0 & -0.0 & -0.0 & 0.0 & -0.0 \\ 0.0 & 0.0 & -0.0 & -0.0 & 0.0 & 0.0 \\ -0.0 & -0.0 & -0.0 & -0.0 & -0.0 & 0.0 \\ -0.0 & -0.0 & 0.0 & -0.0 & 0.0 & -0.0 \end{bmatrix}$$

The state space models of the remaining 4 models are obtained similarly. The characteristics of the smart flexible cantilever beam of the model 1 are given in Table III.

TABLE III
 CHARACTERISTICS OF THE SMART FLEXIBLE BEAM FOR THE
 MULTIVARIABLE MODEL 1

| Models | EIGEN VALUES | Natural Frequency (Hz.) |
|---------|-----------------------|-------------------------|
| Model 1 | $-0.0071 \pm j 9.36$ | 1.4892 |
| | $-0.5975 \pm j 89.2$ | 14.1995 |
| | $-4.96 \pm j 257.1$ | 40.9239 |
| | $-21.3 \pm j 532.1$ | 84.6910 |
| | $-81.2 \pm j 1037.2$ | 165.0721 |
| | $-224.4 \pm j 1715.1$ | 272.9711 |

Similarly, the characteristics of the other 4 models are obtained.

III. DESIGN OF POF CONTROLLER VIA THE REDUCED ORDER MODELING

In the following section, we develop the control strategy for the multivariable cum multimodel representation of the developed smart structure model using the periodic output feedback control law [4]-[6], [15], [26], [27] with 1 actuator input u and 1 sensor output y for the 5 models of the smart

structure plant as shown in Fig. 2. The problem of pole assignment by piecewise constant output feedback was studied by Chammas and Leondes [4]-[6] for LTI systems with infrequent observations. They have shown that by the use of a periodically time-varying piecewise constant output feedback gain, the poles of the discrete time control system could be assigned arbitrarily (within the natural restriction that they should be located symmetrically with respect to the real axis) using the POF technique. Since the feedback gains are piecewise constants, their method could easily be implemented, guarantees the closed loop stability and indicated a new possibility. Such a control law can stabilize a much larger class of systems.

A. Review of Periodic output feedback control technique

Consider a LTI CT system [4]-[6], [27] given by

$$\dot{x} = Ax + Bu, \quad y = Cx, \quad (65)$$

which is sampled with a sampling interval τ secs and given by the discrete linear time invariant system (called as the tau system) as

$$x(k+1) = \Phi_\tau x(k) + \Gamma_\tau u(k), \quad y(k) = Cx(k), \quad (66)$$

where $x \in \mathfrak{R}^n$, $u \in \mathfrak{R}^m$, $y \in \mathfrak{R}^p$ and Φ_τ, Γ_τ and C are constant matrices of appropriate dimensions. The following control law is applied to this system. The output y is measured at the time instant $t = k\tau$, $k = 0, 1, 2, \dots$. We consider constant hold function because they are more suitable for implementation. An output-sampling interval is divided into N sub-intervals of length $\Delta = \tau / N$ and the hold function is assumed to be constant on these sub-intervals as shown in the Fig. 3. Thus, the control law becomes

$$u(t) = K_l y(k\tau),$$

$$(k\tau + l\Delta) \leq k\tau \leq (l+1)\Delta, \quad K_{l+N} = K_l \quad (67)$$

for $l = 0, 1, 2, \dots, (N-1)$. Note that a sequence of N gain matrices $\{K_0, K_1, \dots, K_{N-1}\}$, when substituted in Eq. (67), generates a time-varying piecewise constant output feedback gain $K(t)$ for $0 \leq t \leq \tau$.

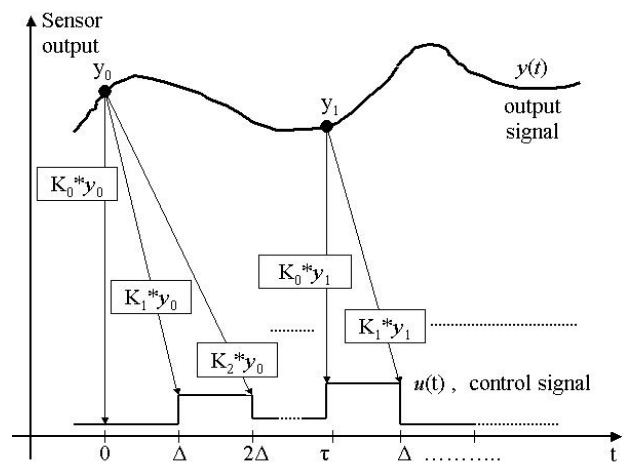


Fig. 3 Graphical illustration of the POF control law

Consider the following system, which is obtained by sampling the system in Eq. (65) at sampling interval of $\Delta = \tau / N$ and denoted by (Φ, Γ, C) called as the delta system :

$$x(k+1) = \Phi x(k) + \Gamma u(k), \quad y(k) = C x(k), \quad (68)$$

A useful property of the control law in Eq. (67) is given by the following lemma which states as "Given an observable pair $(A, B) \in \mathfrak{R}^{(n \times n)} \times \mathfrak{R}^{(n \times m)}$ and $rank(B) = m$, the controllability index of the system w.r.t any particular column of B is the minimum value of ν_i such that the column $A^{\nu_i} B$ is dependent on the columns before it in the following series

$$\{b_1, b_2, \dots, b_m, Ab_1, Ab_2, \dots, Ab_m, \dots, A^{\nu_1} b_1, \dots, A^{\nu_m} b_m, \dots\}, \quad (69)$$

the controllability index of the entire system being defined as $\nu = \max(\nu_i)$ ".

Assume (Φ_τ, C) is observable and (Φ, Γ) is controllable with controllability index ν such that $N \geq \nu$, then it is possible to choose a gain sequence K_l , such that the closed-loop system, sampled over τ , takes the desired self-conjugate set of eigen values [4]-[6], [15], [27]. Define

$$\mathbf{K} = \begin{bmatrix} K_0 \\ K_1 \\ K_2 \\ \vdots \\ K_{N-1} \end{bmatrix}, \quad (70)$$

$$\mathbf{u}(k\tau) = \mathbf{K} y(k\tau) = \begin{bmatrix} u(k\tau) \\ u(k\tau + \Delta) \\ \vdots \\ u(k\tau + \tau - \Delta) \end{bmatrix}, \quad (71)$$

then, a state space representation for the system sampled over τ is

$$x(k\tau + \tau) = \Phi^N x(k\tau) + \Gamma u, \quad y(k) = C x(k), \quad (72)$$

where $\Gamma = [\Phi^{N-1}\Gamma, \dots, \Gamma]$.

Applying POF in Eq. (67), i.e., $\mathbf{K} y(k\tau)$ is substituted for $\mathbf{u}(k\tau)$, the closed loop system becomes

$$x(k\tau + \tau) = (\Phi^N + \Gamma \mathbf{K} C) x(k\tau). \quad (73)$$

The problem has now taken the form of static output feedback [23], [28]. Eq. (73) suggests that an output injection matrix G be found such that

$$\rho(\Phi^N + GC) < 1, \quad (74)$$

where $\rho(\cdot)$ denotes the spectral radius. By observability, one can choose an output injection gain G to achieve any desired self-conjugate set of eigen values for the closed-loop matrix $(\Phi^N + GC)$ and from $N \geq \nu$, it follows that one can find a POF gain which realizes the output injection gain G by

solving

$$\Gamma \mathbf{K} = G \quad (75)$$

for \mathbf{K} . The controller obtained from this equation will give the desired behaviour, but might require excessive control action. To reduce this effect, we relax the condition that \mathbf{K} exactly satisfy the linear equation and include a constraint on it. Thus, we arrive at the following in the inequality equations :

$$\|\mathbf{K}\| < \rho_1, \quad \|\Gamma \mathbf{K} - G\| < \rho_2. \quad (76)$$

Using the schur complement, it is straight forward to bring these conditions in the form of linear matrix inequalities [11], [28] as

$$\begin{bmatrix} -\rho_1^2 I & \mathbf{K} \\ \mathbf{K}^T & -I \end{bmatrix} < 0, \quad \begin{bmatrix} -\rho_2^2 I & (\Gamma \mathbf{K} - G) \\ (\Gamma \mathbf{K} - G)^T & -I \end{bmatrix} < 0. \quad (77)$$

In this form, the LMI toolbox of MATLAB can be used for the synthesis of \mathbf{K} .

B. Multimodel Synthesis

For the multimodel representation of a plant, it is necessary to design a controller that will robustly stabilize the multimodel system. Multimodel representation of plants can arise in several ways. When a non-linear system has to be stabilized at different operating points, linear models are sought to be obtained at those operating points. Even for parametric uncertain linear systems, different linear models can be obtained for extreme points of the parameters. These models are then used for the stabilization of the systems [4]-[6].

Consider a family of plants, $S = \{A_i, B_i, C_i\}$ defined by

$$\dot{x} = A_i x + B_i u, \quad y = C_i x, \quad i = 1, 2, \dots, M. \quad (78)$$

By sampling the above system in (78) at the rate of $1/\Delta$, we get a family of discrete systems $S = \{\Phi_i, \Gamma_i, C_i\}$.

Assume that (Φ_i^N, C_i) are observable. Then, we can find the output injection gains G_i such that $(\Phi_i^N + G_i C_i)$ has the required set of poles. Now, consider the augmented system defined as follows :

$$\tilde{\Phi} = \begin{bmatrix} \Phi_1 & 0 & \dots & 0 \\ 0 & \Phi_2 & \dots & 0 \\ \vdots & \vdots & \ddots & \vdots \\ 0 & 0 & \dots & \Phi_M \end{bmatrix}, \quad \tilde{\Gamma} = \begin{bmatrix} \Gamma_1 \\ \Gamma_2 \\ \vdots \\ \Gamma_M \end{bmatrix}, \quad \tilde{G} = \begin{bmatrix} G_1 \\ G_2 \\ \vdots \\ G_M \end{bmatrix}. \quad (79)$$

The linear equation

$$\begin{bmatrix} \tilde{\Phi}^{N-1} \tilde{\Gamma} & \dots & \dots & \tilde{\Gamma} \end{bmatrix} \begin{bmatrix} K_0 \\ K_1 \\ \vdots \\ K_{N-1} \end{bmatrix} = \tilde{G} \quad (80)$$

has a solution if $(\tilde{\Phi}, \tilde{\Gamma})$ is controllable with controllability index $\tilde{\nu}$ and $N \geq \tilde{\nu}$. This POF gain realizes the designed

G_i for all the plants of the family. It has been shown in [27], that the controllability of the individual plant models generically implies the controllability of the augmented system. The controller obtained from the above equation will produce the desired behaviour, but might require excessive control action. To reduce this gain effect, we relax the condition that Eq. (80) has to be satisfied exactly and include a constraint on the gain. Thus, we consider the following inequalities :

$$\| \mathbf{K} \| < \rho_{1i}, \| \Gamma_i \mathbf{K} - G_i \| < \rho_{2i}, \quad i=1, \dots, M, \quad (81)$$

where ρ_1 and ρ_2 represent the upper bounds on the spectral norms of \mathbf{K} and $(\Gamma \mathbf{K} - G)$ and $M = 5$ respectively.

These 2 objectives have been expressed by the upper bounds on matrix norms and each should be as small as possible. ρ_1 small means low noise sensitivity and ρ_2 small means that the POF controller with gain \mathbf{K} is a good approximation of the original design. It should be noted here that closed loop stability requires $\rho_2 < 1$, i.e., the eigen values which determine the error dynamics must lie within the unit disc. This can be formulated in the framework of LMI as follows :

$$\begin{bmatrix} -\rho_{1i}^2 I & \mathbf{K} \\ \mathbf{K}^T & -I \end{bmatrix} < 0, \begin{bmatrix} -\rho_{2i}^2 I & (\Gamma_i \mathbf{K} - G_i) \\ (\Gamma_i \mathbf{K} - G_i)^T & -I \end{bmatrix} < 0. \quad (82)$$

Here, the LMI toolbox of MATLAB can be used for the design of \mathbf{K} [11], [28]. The RDPOF controller obtained by this method requires only constant gains and is hence easier to implement.

C. Robust Decentralized Periodic Output Feedback

In POF, for multimodel synthesis, the gain matrix is generally full. This results in the control input of each plant being a function of the output of all the plants. Decentralized robust POF control can be achieved by making the off-diagonal elements of $\{K_0, K_1, \dots, K_{N-1}\}$ matrices zero. So, the structure of K_i ($i = 0, 1, 2, \dots, N-1$) matrix is assumed as $K_i = \text{diag}[k_{i11}, k_{i22}, k_{i33}, \dots]$; $i = 0, 1, \dots, N-1$.

With this structure of K_i , the problem can be formulated in the framework of LMI using Eqs. (81) and (82) and the desired matrices obtained. Now, it is evident that the control input of each model of the plant is a function of the output of that plant only and this makes the smart structure controller design using POF a robust decentralized one.

D. Model order reduction technique

For many complex processes or when the modes of a dynamical system are very high, the order of the state matrix may be quite large. It would be difficult to work with these large scale dynamical systems [21] in their original form. In such cases, it is common to study the process by approximating it to a simpler model. These mathematical models correspond to approximating a system by its dominant

pole-zeros in the complex plane. They generally require empirical determination of the system parameters.

Many different methods have been developed to accomplish the purpose by estimating the 'dominant' part of the large system and finding a simpler (or reduced order) system representation that has its behaviour akin to the original system. Here, we discuss the model order reduction technique based on the dominant modes retention. It is usually possible to describe the dynamics of a physical dynamical system by a number of linear differential equations with constant coefficients as

$$\dot{x} = Ax + Bu, \quad y = Cx, \quad (83)$$

where A is a $(n \times n)$ matrix.

The simulation and design of controllers become very cumbersome if the order of the system goes high. One way to overcome this difficulty is to develop a reduced model of the higher order system. One of the well-known techniques is based on dominant eigenvalue retention based on the Davison technique [9], [14]. By this method, a system of higher order can be numerically approximated to one of smaller order. The method suggests that a large $(n \times n)$ system can be reduced to a simpler $(r \times r)$ model ($r \leq n$) by considering the effects of the r most dominant (dominant in the sense of being closest to the instability) eigenvalues alone.

The principle of the method is to neglect the eigen values of the original system that are farthest from the origin and retain only the dominant eigenvalues and hence dominant time constants of the original system in the reduced order model. This implies that the overall behaviour of the approximate system will be very similar to that of the original system since the contribution of the unretained eigenvalues to the system response are important only at the beginning of the response, whereas the eigenvalues retained are important throughout the whole of the response. For the system represented by the Eq. (83), consider the linear transformation,

$$x = Pz, \quad (84)$$

which transforms the model Eq. (83) into the following form,

$$\dot{z} = \hat{A}z + \hat{B}u, \quad y = \hat{C}z, \quad (85)$$

where \hat{A} is a $(r \times r)$ matrix and

$$\hat{A} = P^{-1}AP, \quad \hat{B} = P^{-1}B \quad \text{and} \quad \hat{C} = CP. \quad (86)$$

Here, \hat{A} is in the diagonal form as

$$\hat{A} = \text{diag}[\lambda_1, \lambda_2, \dots, \lambda_n] \quad (87)$$

and $\text{Re}(\lambda_1) \geq \text{Re}(\lambda_2) \geq \dots \geq \text{Re}(\lambda_n)$. (88)

Further, assume that only r eigenvalues are dominant, i.e., the order of the reduced model is r and partition the model in Eq. (85) as

$$\dot{z}_1 = \hat{A}_1 z_1 + \hat{B}_1 u, \quad \dot{z}_2 = \hat{A}_2 z_2 + \hat{B}_2 u, \quad y = \hat{C}_1 z_1 + \hat{C}_2 z_2 \quad (89)$$

where

$$\hat{A}_1 = \text{diag}[\lambda_1, \lambda_2, \dots, \lambda_r], \quad \hat{A}_2 = \text{diag}[\lambda_{r+1}, \lambda_{r+2}, \dots, \lambda_n], \quad (90)$$

$\hat{B}_1 =$ first r rows of \hat{B} , $\hat{B}_2 =$ remaining $(n-r)$ rows of \hat{B}

and are respectively $(r \times r)$, $(n-r) \times (n-r)$, $(r \times m)$ and $(n-r) \times m$ matrices obtained by portioning of \hat{A} and \hat{B} suitably. In Eq. (89), the order of z_1 is r and that of z_2 is $(n-r)$. Now, because the contribution of the modes represented by the eigenvalues $\lambda_{r+1}, \lambda_{r+2}, \dots, \lambda_n$ is not significant, it may be assumed that $z_2 = 0$, whereby we have from Eq. (84),

$$\begin{bmatrix} x_1 \\ x_2 \end{bmatrix} = \begin{bmatrix} P_{11} \\ P_{21} \end{bmatrix} z_1, \quad (91)$$

where P_{11} and P_{21} are respectively, $(r \times r)$ and $(n-r) \times r$ submatrices obtained by portioning of P_1 and z_1, z_2 are respectively, r and $(n-r)$ dimensional state vectors corresponding to the original state variables. It follows from Eq. (91) that

$$z_1 = P_{11}^{-1} x_1, \quad (92)$$

with which the model in Eq. (89) can be transformed to

$$\begin{aligned} \dot{x}_1 &= P_{11} \hat{A}_1 P_{11}^{-1} x_1 + P_{11} \hat{B} u = A_x x_1 + B_r u \\ y &= \hat{C}_1 P_{11}^{-1} x_1 = C_r x_1 \end{aligned} \quad (93)$$

Moreover, from Eqns. (91), and (92), we have

$$x_2 = P_{21} P_{11}^{-1} x_1. \quad (94)$$

Thus, the original n^{th} order model represented by Eq. (83) is reduced to an r^{th} order model given by Eq. (93). The state variables of the approximate model are the same as the first r state variables of the original higher-order model. The remaining state variables are given in terms of the first r state variables by Eq. (94).

E. RDPOF Control Design via reduced order model for multimodel system

Let us consider a family of plants $S = \{A_i, B_i, C_i\}$ defined by

$$\dot{x} = A_i x + B_i u, \quad y = C_i x, \quad i = 1, 2, \dots, M. \quad (95)$$

The discrete time invariant systems with sampling interval τ seconds can be represented as

$$x(k+1) = \Phi_{\tau i} x(k) + \Gamma_{\tau i} u(k), \quad y(k) = C_i x(k). \quad (96)$$

The adjoint or the dual for the above systems would be

$$\hat{x}(k+1) = \Phi_{\tau i}^T \hat{x}(k) + C_i^T \hat{u}(k), \quad \hat{y}(k) = \Gamma_{\tau i}^T \hat{x}(k). \quad (97)$$

There exists a transformation V_i , such that,

$$\hat{x} = V_i \hat{z} \quad (98)$$

transforms the above system in Eq. (97) into the following block diagonal modal form as

$$\hat{z}(k+1) = \hat{\Phi}_i \hat{z}(k) + \hat{C}_i \hat{u}(k), \quad \hat{y}(k) = \hat{\Gamma}_i \hat{z}(k), \quad (99)$$

where

$$\hat{\Phi}_i = \begin{bmatrix} \Phi_{1i} & 0 \\ 0 & \Phi_{2i} \end{bmatrix}, \quad \hat{C}_i = \begin{bmatrix} C_{1i} \\ C_{2i} \end{bmatrix}, \quad \hat{\Gamma}_i = \begin{bmatrix} \Gamma_{1i} & \Gamma_{2i} \end{bmatrix} \quad (100)$$

and the eigen values are arranged in the order of their dominance. We now extract an r^{th} order model, retaining the r dominant eigen values, by truncating the above systems. Using Eqns. (99) and (100), we get

$$\hat{z}_r(k+1) = \Phi_{1i} \hat{z}_r(k) + C_{1i} \hat{u}(k), \quad \hat{y}_r(k) = \Gamma_{1i} \hat{z}_r(k). \quad (101)$$

Let $\hat{u}(k) = S_{ri} \hat{z}_r$ be a stabilizing control for the reduced order model in Eq. (101). Thus, the closed loop reduced model $(\Phi_{1i} + C_{1i} S_{ri})$ becomes stable. Now,

$$\hat{Z}_r = \begin{bmatrix} I_r & 0 \\ 0 & 0_{r^*(n-r)} \end{bmatrix} \hat{z} = \begin{bmatrix} I_r & 0 \\ 0 & 0_{r^*(n-r)} \end{bmatrix} V_i^{-1} \hat{x}. \quad (102)$$

\therefore , we get,

$$u(k) = S_{ri} \begin{bmatrix} I_r & 0 \\ 0 & 0_{r^*(n-r)} \end{bmatrix} V_i^{-1} \hat{x} = S_i \hat{x} \quad (103)$$

which makes the closed loop system $(\Phi_{\tau i}^T + C_i^T S_i)$ stable.

But the eigen values of $(\Phi_{\tau i}^T + C_i^T S_i)$ and $(\Phi_{\tau i}^T + C_i^T S_i)^T$ are the same. So, $(\Phi_{\tau i}^T + S_i^T C_i)$ will also be stable. Thus,

$S_i^T \equiv G_i$ is the output injection gain for the system in Eq. (96). Using these output injection gains G_i , the following inequalities are solved.

$$\|\mathbf{K}\| < \rho_{1i}, \quad \|\Gamma_i \mathbf{K} - G_i\| < \rho_{2i}, \quad i = 1, \dots, M. \quad (104)$$

The controller obtained from the above equation will give desired behaviour, but might require excessive control action. To reduce this effect, we relax the condition that \mathbf{K} exactly satisfy the above linear equation and include a constraint on the gain \mathbf{K} . Thus, this can be formulated in the framework of Linear Matrix Inequalities (LMI) as given in the following equation

$$\begin{bmatrix} -\rho_{1i}^2 I & \mathbf{K} \\ \mathbf{K}^T & -I \end{bmatrix} < 0, \quad \begin{bmatrix} -\rho_{2i}^2 I & (\Gamma_i \mathbf{K} - G_i) \\ (\Gamma_i \mathbf{K} - G_i)^T & -I \end{bmatrix} < 0. \quad (105)$$

Here, the LMI toolbox of MATLAB can be used for the design of \mathbf{K} [11], [28]. If the LMI constraints given in Eqns. (104) and (105) are solved using the above G_i , the robust periodic output feedback gain matrix may become full. This results in the control input of each model being a function of the outputs of all the models. To obtain the RDPOF control, the off-diagonal elements of K_0, K_1, \dots, K_{N-1} matrices are made equal to zero as a result of which the control input to each actuator is a function of the output of that corresponding sensor only. This makes the POF control technique a robust decentralized one and is more feasible.

IV. CONTROL SIMULATIONS OF THE SMART BEAM

The finite element and the state space model of the smart cantilever beam is developed in MATLAB using Euler-Bernoulli beam theory. The flexible cantilever beam is divided into 4 finite elements and the sensor and actuator as collocated pairs at finite element positions 2 and 4 respectively, thus giving rise to a multivariable beam with 2 inputs and 2 outputs. By varying the thickness of the beam from 0.5, 0.6,

0.7, 0.8 and 1 mm, 5 multivariable models are obtained. These 5 MIMO models give rise to a multimodel smart structure plant. A 12th order state space model of the system is obtained on retaining the first 6 modes of vibration of the system. Simulations are carried out in MATLAB.

The POF control techniques discussed in the previous sections is used to design a controller to suppress the 1st 6 vibration modes of a cantilever beam through the smart structure concept for the various multivariable models of the smart beam. RDPOF feedback based reduced model order controller is designed for multimodel smart structure system using the developed multivariable state space model and its performance is evaluated for the Active Vibration Control.

The first task in designing the POF controller is the selection of the sampling interval τ . The maximum bandwidth for all the sensor / actuator locations on the beam are calculated (here, the 6th vibratory mode of the plant) and then by using existing empirical rules for selecting the sampling interval based on bandwidth, approximately 10 times of the maximum 6th vibration mode frequency of the system has been selected. The sampling interval used is $\tau = 0.004$ seconds. The number of sub-intervals N is chosen to be 10.

An external force \mathbf{f}_{ext} of 1 Newton is applied for duration of 50 ms at the free end of the beam for all the 5 models of the Fig. 2. RDPOF Controllers via the reduced order modeling has been designed to control the first 6 modes of vibration of the smart cantilever beam for the 5 models of the smart structure. A large 12th order system of (12×12) is reduced to a simpler 6th order model of (6×6) , by considering the effects of the 6 most dominant (dominant in the sense of being closed to instability) eigen values. The eigen values of the original system that are farthest from the origin are neglected and only dominant eigen values of the original system in the reduced order model is retained. The open loop and closed loop responses of the system are observed.

The periodic output feedback gain matrix \mathbf{K} for the system given is obtained by solving $\mathbf{\Gamma K} = \mathbf{G}$ using the LMI optimization method [11], [28] which reduces the amplitude of the control signal \mathbf{u} . For convenience, only the closed loop impulse responses (sensor outputs y_1 and y_2) with RDPOF feedback gain \mathbf{K} of the system and the variation of the control signal u_1 and u_2 with time for the multivariable-multimodel system are shown in Figs. 4 - 13 respectively.

The 5 multivariable models of the smart structure system are considered for designing the RDPOF feedback controller via the reduced order model using the LMI technique approach of MATLAB. The discrete models are obtained for sampling time of $\tau = 0.004$ seconds. The reduced order models are computed from the adjoint discrete models discussed in the previous sections. Using the method discussed in the previous sections, stabilizing gain matrices S_{r_i} is obtained for the reduced order model using the DLQR

theory.

Using aggregation techniques [1], the output injection gain G_i can be calculated for the higher order (actual) models. This POF gain can be obtained which approximately realizes the designed G_i for all the models of the family. Here, as we are dealing with robust stabilization, we have to find a \mathbf{K} which will satisfy $\mathbf{\Gamma}_i \mathbf{K} = G_i$, ($i = 1$ to 5) all these equations using the LMI approach. The gain sequences of \mathbf{K} are chosen 10 $(K_1, K_2, \dots, K_{10})$. In our problem considered $N = 10$ had given good results. Using the output injection gains G_i , LMI constraints given in Eqns. (104) and (105) are solved for different values of ρ_1 and ρ_2 to find the robust decentralized gain matrix \mathbf{K} for the actual models via the reduced order model.

The closed loop responses with this RDPOF feedback gain \mathbf{K} via the reduced order model for all the models are satisfactory and are able to stabilize the outputs. The eigen values of $(\Phi^N + \mathbf{G C})$ are found to be within the unit circle. It is found that the designed robust decentralized FOS feedback controllers via the reduced order model provided good damping enhancement for the various multivariable models of the smart structure plant.

The proposed robust decentralized control for the multimodel smart structure system can be applied simultaneously to all the models and results in satisfactory response behaviour to damp out the vibrations, which can be seen from the simulation results in section 5. The input applied to each actuator of the model is a function of the output of that respective sensor only, which makes the control technique a robust, decentralized one. The RDPOF gain is

$$\mathbf{K} = 10^2 * \begin{bmatrix} -1.6410 & 0 \\ 0 & 0.0173 \\ 0.2375 & 0 \\ 0 & -0.0148 \\ 1.1130 & 0 \\ 0 & -0.0212 \\ 0.6873 & 0 \\ 0 & -0.0040 \\ -0.4794 & 0 \\ 0 & 0.0177 \\ -0.8435 & 0 \\ 0 & 0.0122 \\ 0.4678 & 0 \\ 0 & -0.0217 \\ 0.0804 & 0 \\ 0 & 0.0084 \\ -0.0489 & 0 \\ 0 & -0.0027 \\ 0.0035 & 0 \\ 0 & 0.0003 \end{bmatrix} \quad (106)$$

(20×2)

V. SIMULATION RESULTS

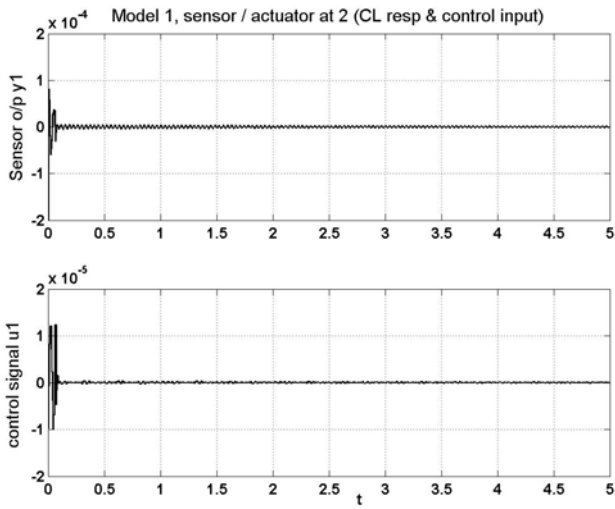


Fig. 4 CL response and control input (sensor / actuator placed at FE 2) : Model 1

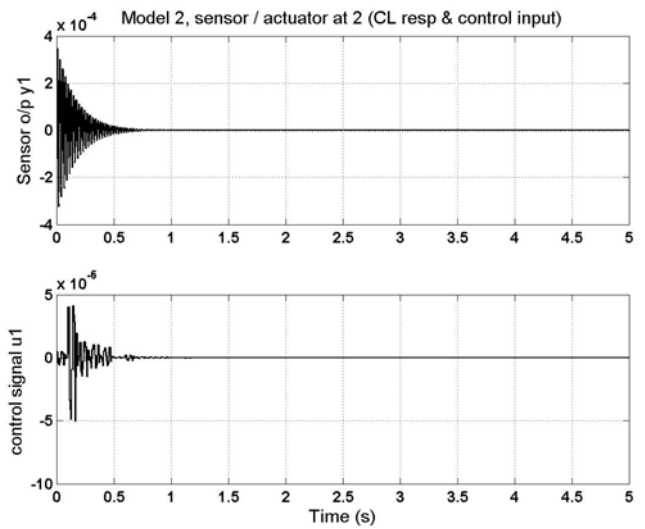


Fig. 6 CL response and control input (sensor / actuator placed at FE 2) : Model 2

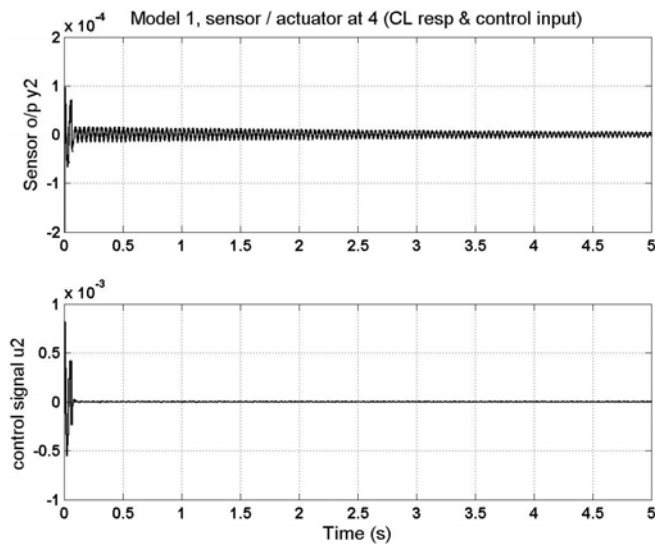


Fig. 5 CL response and control input (sensor / actuator placed at FE 4) : Model 1

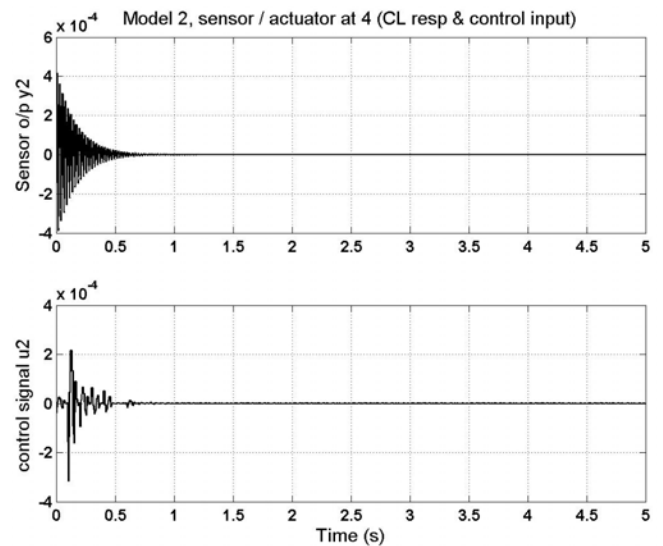


Fig. 7 CL response and control input (sensor / actuator placed at FE 4) : Model 2

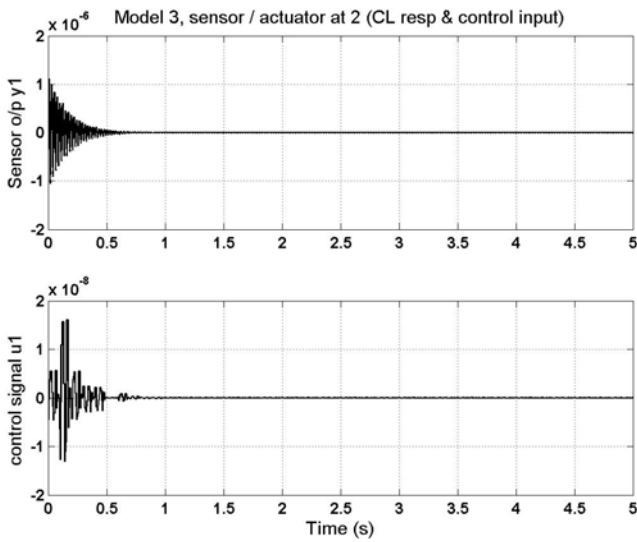


Fig. 8 CL response and control input (sensor / actuator placed at FE 2) : Model 3

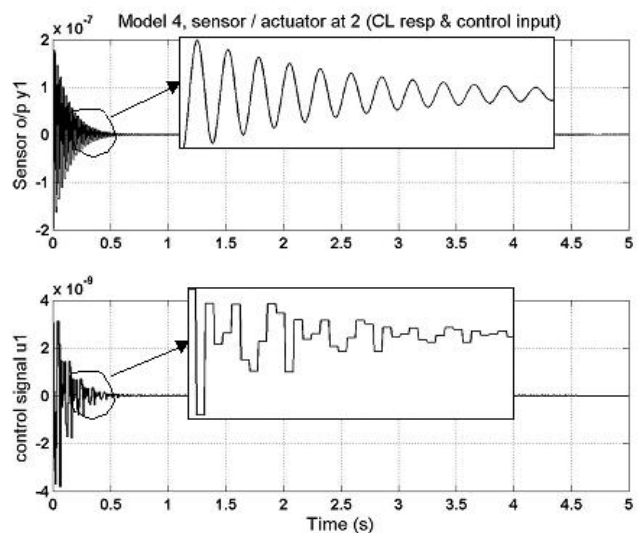


Fig. 10 CL response and control input (sensor / actuator placed at FE 2) : Model 4

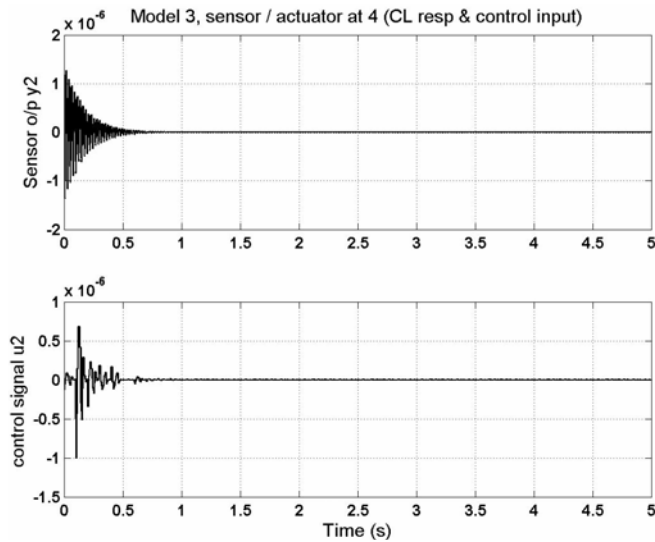


Fig. 9 CL response and control input (sensor / actuator placed at FE 4) : Model 3

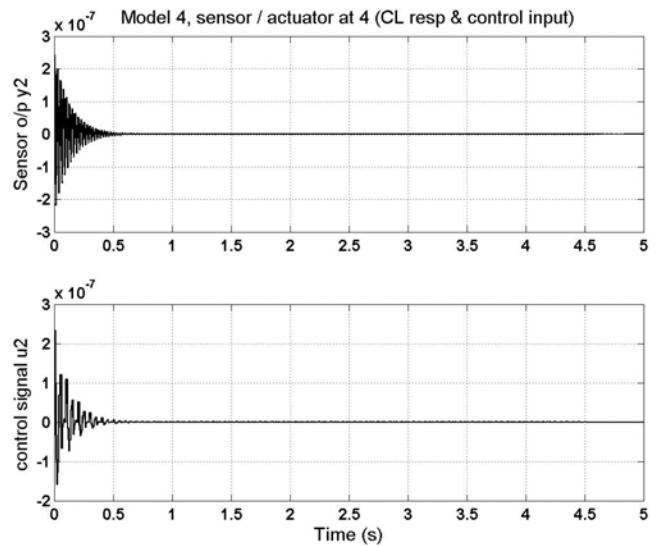


Fig. 11 CL response and control input (sensor / actuator placed at FE 4) : Model 4

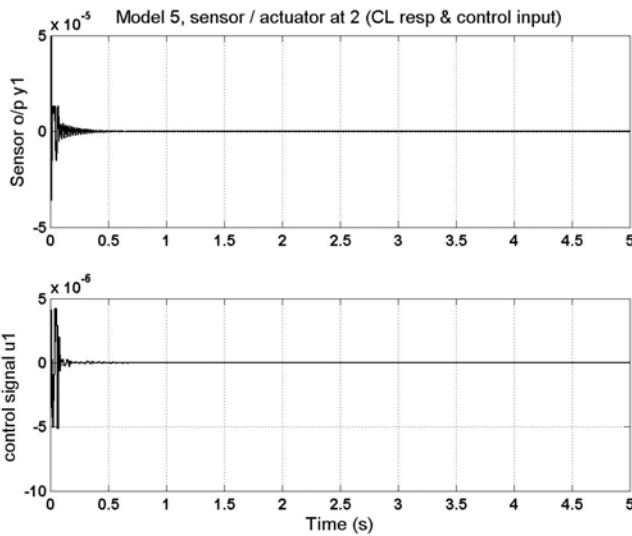


Fig. 12 CL response and control input (sensor / actuator placed at FE 2) : Model 5

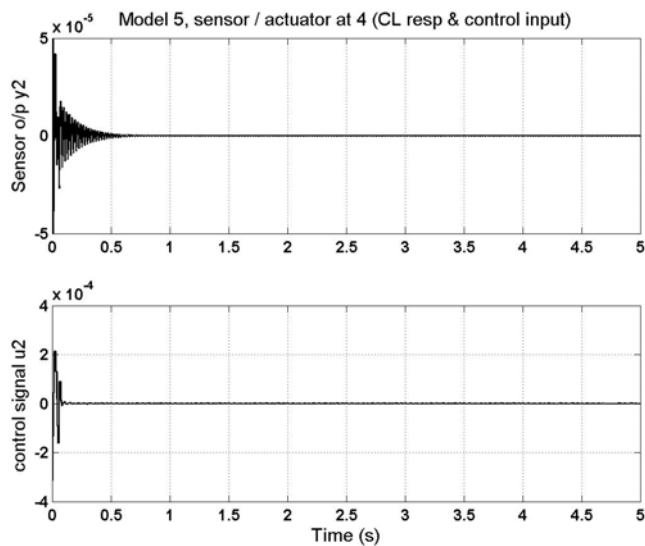


Fig. 13 CL response and control input (sensor / actuator placed at FE 4) : Model 5

VI. CONCLUSIONS

Robust Decentralized Periodic Output Feedback Controller is designed and proposed for the multivariable smart structure using the various models of the single plant via the reduced order modeling. Simulations are done in Matlab and the various responses are obtained for the designed state space based FE model of the smart flexible cantilever beam. Through the simulation results, it is shown that when the plant is placed with the designed robust decentralized POF controller, the s models performs well and the stability is guaranteed.

In the control law, the control input to each actuator of the multivariable plant's multimodel is a function of the output of that corresponding sensor only and the gain matrix has got all off-diagonal elements zero. This makes the POF control technique a robust decentralized one. This would render better control and is more feasible. The robust decentralized POF

controller designed by the above method requires only constant gains and hence is easier to implement. Closed loop responses are simulated for the various multivariable models of the smart structure plant.

A new algorithm is proposed for the design of robust decentralized controllers for a multivariable system using POF feedback technique via the reduced order model. The computation of the output injection gain, which is needed to obtain the decentralized POF feedback based smart structure system, becomes very tedious when a number of modes, especially greater than 5 are considered. Here, a output injection gain is computed from the reduced order model of the smart system and using the aggregation techniques, a output injection gain can be obtained for the higher order (actual model). The simulation results shows the effectiveness of the proposed method.

The RDPOF feedback gain which realizes this output injection gain, can be obtained for the actual model. It is found that the designed and proposed robust controller via the reduced order model provides good damping enhancement for the models of the smart structure system. Thus, an integrated finite element model to analyze the vibration suppression capability of a smart cantilever beams with surface mounted piezoelectric devices based on Euler-Bernoulli beam theory and reduced order modeling is proposed in this paper.

ACRONYMS / ABBREVIATIONS

| | |
|------|---|
| SISO | Single Input Single Output |
| FEM | Finite Element Method |
| FE | Finite Element |
| LMI | Linear Matrix Inequalities |
| MR | Magneto Rheological |
| ER | Electro Rheological |
| PVDF | Poly Vinylidene Fluoride |
| SMA | Shape Memory Alloys |
| CF | Clamped Free |
| CC | Clamped-Clamped |
| CT | Continuous Time |
| DT | Discrete Time |
| OL | Open Loop |
| CL | Closed Loop |
| HOBT | Higher Order Beam Theory |
| LTI | Linear Time Invariant |
| FOS | Fast Output Sampling |
| AVC | Active Vibration Control |
| EB | Euler-Bernoulli |
| PZT | Lead Zirconate Titanate |
| DOF | Degree Of Freedom |
| IEEE | Institute of Electrical & Electronics Engineers |

NOMENCLATURE (LIST OF SYMBOLS)

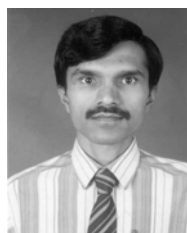
| | |
|-----------|----------------------|
| f_{ext} | External force input |
| l_b | Length of the beam |
| b | Width of the beam |

| | | | |
|--------------------------|---|--|---|
| E_b | Young's modulus of beam | K_c | Controller gain K_c |
| ρ, ρ_b | Mass density of beam | \mathbf{p}^T | Constant vector, which depends |
| α, β | Structural constants | \mathbf{h}^T | Constant vector, depends on sensor / actuator characteristics |
| t_b | Thickness of beam | $V^a(t)$ | Actuator voltage |
| t_a | Thickness of actuator | $V^s(t)$ | Sensor voltage |
| t_s | Thickness of sensor | M_A | Resultant moment acting on the beam |
| ρ_p | Mass density of piezoelectric | \mathbf{f}_{ctrl} | Control force applied by the actuator because of electric field |
| θ X, Y and Z | The 3 axis of 3D space | \mathbf{f}^t | Total force coefficient vector |
| \dot{w} | Linear velocity | \mathbf{T} | Modal matrix containing eigenvectors representing the 1 st 6 modes |
| W | External work done | \mathbf{M}^* | Generalized mass matrix |
| t | Time in secs | \mathbf{K}^* | Generalized stiffness matrix |
| d_{31} | Piezoelectric strain constant | \mathbf{f}_{ext}^* and \mathbf{f}_{ctrl}^* | Generalized external force vector and generalized control force vector |
| g_{31} | Piezoelectric stress constant | \mathbf{C}^* | Generalized damping matrix |
| θ | Bending angle (rotation about Y axis) | \mathbf{g} | Principal coordinates |
| E_p | Young's modulus of piezoelectric | $u(t)$ | Control input |
| w | Time dependent transverse displacement of Z axis | $r(t)$ | External input to the system |
| l_p | Length of the piezoelectric patch | $y(t)$ | Output of the system, i.e., sensor output |
| I | Mass moment of inertia of the beam element | $x(t)$ | State vector |
| A | Area of cross section of beam element | $\mathbf{A}, \mathbf{B}, \mathbf{C}, \mathbf{D}$ | State space matrices (CT) : System, input, output, transmission matrix |
| T, U | Kinetic energy and strain energy | \mathbf{E} | External load matrix, which couples the disturbance to the system |
| a_i ($i=1, 2, 3, 4$) | Unknown coefficients | $\dot{x}(t)$ | Derivative of the state vector |
| b_j ($j=1, 2, 3$) | Unknown coefficients | \mathfrak{R}^n | n dimension space |
| \mathbf{q} | Vector of displacements and slopes | τ | Sampling interval in seconds |
| $\dot{\mathbf{q}}$ | Strain rate | $\mathbf{C}_0, \mathbf{D}_0$ | Lifted system matrices |
| K^b | Stiffness matrix of regular beam element (local stiffness matrix) | Φ_τ, Γ_τ | System matrix, input matrix discretized at sampling interval of τ secs |
| M^b | Mass matrix of the regular beam element (local mass matrix) | Φ, Γ | System matrix, input matrix discretized at sampling interval of Δ secs |
| K^p | Stiffness matrix (local) of piezoelectric beam element | G | Output injection gain |
| M^p | Mass matrix (local) of piezoelectric element | \mathcal{U} | Controllability index of the system |
| A_p | Area of the piezoelectric patch | u_k, y_k | Input and output at the k^{th} instant |
| E_f | Electric field | \mathbf{K} | POF gain matrix |
| \mathbf{M}, \mathbf{K} | Mass & stiffness of regular beam element, assembled matrices (global) | ρ_1, ρ_2 | Spectral norms |
| D | Dielectric displacement | \mathbf{I} | Identity matrix |
| e | Permittivity of the medium | | |
| s^E | Compliance of the medium | | |
| d | Piezoelectric constant | | |
| $Q(t)$ | Charge developed on the sensor surface | | |
| $i(t)$ | Current generated by the sensor surface (due to the strain) | | |
| e_{31} | Piezoelectric stress / charge constant | | |
| V^s | Sensor voltage V^s | | |
| G_c | Signal-conditioning device with gain | | |

REFERENCES

- [1] M. Aoki, "Control of large scale dynamic systems by aggregation," *IEEE Trans. Auto. Contr.*, vol. AC-13, pp. 246 - 253, 1968.
- [2] T. Baily, and J. E. Hubbard Jr., "Distributed piezoelectric polymer active vibration control of a cantilever beam", *J. of Guidance, Control and Dynamics*, vol. 8, pp. 605 - 611, 1985.
- [3] E. F. Crawley, and J. De Luis, "Use of piezoelectric actuators as elements of intelligent structures," *AIAA J*, vol. 25, pp. 1373 - 1385, 1987.

- [4] A. B. Chammas, and C. T. Leondes, "Pole placement by piecewise constant output feedback," *Int. J. Contr.*, vol. 29, pp. 31 - 38, 1979.
- [5] A. B. Chammas, and C. T. Leondes, "On the design of LTI systems by periodic output feedback, Part-I, Discrete Time pole assignment," *Int. J. Ctrl.*, vol. 27, pp. 885 - 894, 1978.
- [6] A. B. Chammas, and C. T. Leondes, "On the design of LTI systems by periodic output feedback, Part-II, Output feedback controllability," *Int. J. Ctrl.*, vol. 27, pp. 895 - 903, 1978.
- [7] B. Culshaw, "Smart Structures : A concept or a reality," *J. of Systems and Control Engg.*, vol. 26, no. 206, pp. 1 - 8, 1992.
- [8] S. B. Choi, C. Cheong, and S. Kini, "Control of flexible structures by distributed piezo-film actuators and sensors," *J. of Intelligent Materials and Structures*, vol. 16, pp. 430 - 435, 1995.
- [9] E. J. Davison, "A method for simplifying linear dynamical systems," *IEEE Trans. Auto. Contr.*, vol. AC-11, pp. 93 - 101, 1966.
- [10] J. L. Fanson, and T. K. Caughey, "Positive position feedback control for structures," *AIAA J.*, vol. 18, no. 4, pp. 717 - 723, 1990.
- [11] P. Gahnet, A. Nemirovski, A. J. Laub, and M. Chilali, "LMI Tool box for Matlab", *The Math works Inc., Natick MA*, 1995.
- [12] W. Hwang, and H. C. Park, "Finite element modeling of piezoelectric sensors and actuators", *AIAA J.*, vol. 31, no. 5, pp. 930 - 937, 1993.
- [13] S. Hanagud, M. W. Obal, and A. J. Callise, "Optimal vibration control by the use of piezoceramic sensors and actuators," *J. of Guidance, Control and Dyn.*, vol. 15, no. 5, pp. 1199 - 1206, 1992.
- [14] S. S. Lamba, and S. Vittal Rao, "On the suboptimal control via the simplified model of Davison," *IEEE Trans. Auto. Contr.*, vol. AC-19, pp. 448 - 450, 1974.
- [15] W. S. Levine, and M. Athans, "On the determination of the optimal constant output feedback gains for linear multivariable systems," *IEEE Trans. Auto. Contr.*, vol. AC-15, pp. 44 - 48, 1970.
- [16] J. Mark Balas, "Feedback control of flexible structures," *IEEE Trans. Automat. Contr.*, vol. AC-23, pp. 673 - 679, 1978.
- [17] T. C. Manjunath, and B. Bandyopadhyay, "Vibration control of a smart flexible cantilever beam using periodic output feedback control technique," *Proc. Fourth Asian Control Conference ASCC-2002*, paper no. 1679, pp. 1302 - 1307, Sept. 25-27, 2002.
- [18] T. C. Manjunath, and B. Bandyopadhyay, "Vibration control of a smart flexible cantilever beam using periodic output feedback," *Asian Journal of Control*, vol. 6, no. 1, pp. 74 - 87, Mar. 2004.
- [19] T. C. Manjunath, and B. Bandyopadhyay, "Fault tolerant control of flexible smart structures using robust decentralized periodic output sampling feedback technique," *International Journal of Smart Mater. and Struct.*, vol. 14, no. 4, pp. 624 - 636, Aug. 2005.
- [20] T. C. Manjunath, and B. Bandyopadhyay, R. Gupta, and M. Umamathy, "Multivariable control of a smart structure using periodic output feedback control technique," *Proc. of the Seventh International Conference on Control, Automation, Robotics and Computer Vision, ICARCV 2002, Singapore*, Paper No. 2002P1283, pp. 1481-1486, Dec. 2-5, 2002.
- [21] M. S. Mahmoud, and G. M. Singh, "Large scale systems modeling," *Pergamon Press*, Oxford, 1981.
- [22] S. Rao, and M. Sunar, "Piezoelectricity and its uses in disturbance sensing and control of flexible structures : A survey," *Applied Mechanics Rev.*, vol. 47, no. 2, pp. 113 - 119, 1994.
- [23] V. L. Syrmos, P. Abdallah, P. Dorato, and K. Grigoriadis, "Static output feedback : A survey," *Automatica*, vol. 33, no. 2, pp. 125 - 137, 1997.
- [24] P. Seshu, "Textbook of Finite Element Analysis," 1st Ed. Prentice Hall of India, New Delhi, 2004.
- [25] M. Umamathy, and B. Bandyopadhyay, "Control of flexible beam through smart structure concept using periodic output feedback," *System Science Journal*, vol. 26, no. 1, pp. 23 - 46, 2000.
- [26] H. Werner, and K. Furuta, "Simultaneous stabilization based on output measurements," *Kybernetika*, vol. 31, no. 4, pp. 395 - 411, 1995.
- [27] H. Werner, "Robust multivariable control of a turbo-generator by periodic output feedback," vol. 31, no. 4, pp. 395 - 411, 1997.
- [28] Y. C. Yan, J. Lam, and Y. X. Sun, "Static output feedback stabilization: An LMI approach," *Automatica*, vol. 34, no. 12, pp. 1641 - 1645, 1998.



T. C. Manjunath, born in Bangalore, Karnataka, India on Feb. 6, 1967 received the B.E. Degree in Electrical Engineering from the University of Bangalore in 1989 in First Class and M.E. in Electrical Engineering with specialization in Automation, Control and Robotics from the University of Gujarat in 1995 in First Class with Distinction, respectively. He has got a teaching experience of 17 long years in various engineering colleges all over the country and is currently working as a Research Engineer in the department of systems and control engineering, Indian Institute of Technology Bombay, India and simultaneously doing his Ph.D. in the Interdisciplinary Programme in Systems and Control Engineering, Indian Institute of Technology Bombay, Powai, Mumbai-400076, India, in the field of modeling, simulation, control and implementation of smart flexible structures using DSpace and its applications. He has published 67 papers in the various national, international journals and conferences and published two textbooks on Robotics, one of which has gone upto the third edition and the other, which has gone upto the fourth edition along with the CD which contains 200 C / C++ programs for simulations on robotics. He is a student member of IEEE since 2002, SPIE student member and IOP student member since 2004, life member of ISSS, life member of Systems Society of India and a life member of the ISTE, India. His biography was published in 23rd edition of Marquis' Who's Who in the World in 2006 issue. He has also guided more than 2 dozen robotic projects. His current research interests are in the area of Robotics, Smart Structures, Control systems, Network theory, Mechatronics, Process Control and Instrumentation, CT and DT signals and systems, Signal processing, Periodic output feedback control, Fast output feedback control, Sliding mode control of SISO and multivariable systems and its applications.



B. Bandyopadhyay, born in Birbhum village, West Bengal, India, on 23rd August 1956 received his Bachelor's degree in Electronics and Communication Engineering from the University of Calcutta, Calcutta, India, and Ph.D. in Electrical Engineering from the Indian Institute of Technology, Delhi, India in 1978 and 1986, respectively. In 1987, he joined the Interdisciplinary Programme in Systems and Control Engineering, Indian Institute of Technology Bombay, India, as a faculty member, where he is currently a Professor. He visited the Center for System Engineering and Applied Mechanics, Universite Catholique de Louvain, Louvain-la-Neuve, Belgium, in 1993. In 1996, he was with the Lehrstuhl fur Elektrische Steuerung und Regelung, Ruhr Universitat Bochum, Bochum, Germany, as an Alexander von Humboldt Fellow. He revisited the Control Engineering Laboratory of Ruhr University of Bochum during May-July 2000. He has authored and coauthored 7 books and book chapters, 56 national and international journal papers and 123 conference papers, totaling to 186 publications. His research interests include the areas of large-scale systems, model reduction, nuclear reactor control, smart structure control, periodic output feedback control, fast output feedback control and sliding mode control. Prof. Bandyopadhyay served as Co-Chairman of the International Organization Committee and as Chairman of the Local Arrangements Committee for the IEEE International Conference in Industrial Technology, held in Goa, India, in Jan. 2000. His biography was published in Marquis' Who's Who in the World in 1997. Prof. B. Bandyopadhyay has been nominated as one of the General Chairmen of IEEE ICIT conference to be held in Mumbai, India in December 2006 and sponsored by the IEEE Industrial Electronics Society.